Robotica (2002) volume 20, pp. 439–446. © 2002 Cambridge University Press
DOI: 10.1017/S0263574702004113 Printed in the United Kingdom

Control of an operator-assisted mobile robotic system

Jae H. Chung

Department of Mechanical Engineering, Stevens Institute of Technology, Castle Point on Hudson, Hoboken, NJ 07030 (USA)

(Received in Final Form: February 16, 2002)

SUMMARY

In this paper, two different control methods are developed for an operator-assisted mobile robotic system for high load applications. For high load applications of mobile robots, an accurate tire model that considers wheel slip needs to be studied to achieve robustness of the system response. First, a simple operator-manipulator coordination system is developed based on explicit force control. Then, a position controller for the platform is designed to minimize the effect of wheel slip on control performance and integrated with the force controller for the operator-manipulator subsystem based on a motion coordination scheme. Then, a new type of human-robot coordination control method is developed, in which robust force control of the manipulator and impedance control of the mobile platform are integrated to achieve robust response and smooth interaction between the operator, the manipulator and the mobile platform. In simulation, the developed methods are compared for control performance on following the operator's motion intention.

KEYWORDS: Mobile system; Operator-assist; High loads; Tire model.

1. INTRODUCTION

A mobile manipulator consists of a manipulator that is mounted upon a mobile platform. In recent years, interest in the area of mobile manipulators has increased significantly due to their mobility and dexterity. Mobilizing the manipulator almost always results in kinematic redundancy increasing the dexterous manipulation of the end effector. This enables the manipulator to perform a broader range of tasks. Consequently, interest in applying mobile manipulators to industrial, military, and public service applications grow annually.

Until recently, much research in the area of motion control of mobile robotic systems was aimed at fully automated operation. However, for different reasons such as algorithm complexity, safety, and impossibility of modeling the full environment surrounding them, semi-automated systems combining human operation with some automatic features, will be more promising, which will avoid dealing with highly complex and unsolved control problems for which human skill is better adapted.

Much research has been done on fixed-base manipulators with human interaction, such as Hardyman, a master-slave manipulator system, a robot for man-robot cooperation, an Extender, etc. Fukuda et al.[1] have proposed a manipulator, which is designed for handling heavy objects in cooperation with a human. Kazerooni[2] proposed the extender or the manipulator system to extend the strength of the human arm. Also, there exists a limited amount of literature that considers human factors. Al-Jarrah[3] investigated the arm-manipulation coordination problem using a compliant control method. In reference [4], a control method was proposed for a mechanical system having direct mechanical interaction with an environment and an operator. Yamamoto's paper[5] is the only research work available in the area of human/mobile manipulator coordination control. He developed a force control scheme in order for a mobile manipulator to sustain an object. However, the complexity of the modeling and control problem is excessively simplified such that the human intention represented by the reference trajectory and the actual trajectory are identical, which means perfect position and force control that would never be achieved even for low speed tasks.

In this paper, two different control methods for an operator-mobile manipulator coordination system (OMMCS) are developed for high-load applications, in which a dynamic model of the wheeled mobile platform is considered to include the effect of wheel slip that acts as a disturbance to the system. First, a simple operator-manipulator coordination system is developed based on robust force control. The developed control method is verified experimentally for the coordination system. Then, a position-based robust platform controller is designed to achieve the objective of minimizing the effect of wheel slip on control performance. The developed controllers for the subsystems, the operator-manipulator and the platform, are integrated based on the coordination algorithm developed in reference [6]. Then, a new type of coordination control called the interactive force control scheme is developed to achieve for the OMMCS based on the study of the simple operator-manipulator coordination system and a base force/torque sensor. In the interactive force control scheme, robust force control of the manipulator and impedance control of the mobile platform are integrated to achieve nondestructive interaction between the operator, the manipulator and the mobile platform and, subsequently, to minimize the harmful effect of wheel slip on control performance. The developed control methods are compared in terms of tracking. Simulation results show the superior performance of the interactive force controller that utilizes impedance control based on a base force/torque sensor.

https://doi.org/10.1017/S0263574702004113 Published online by Cambridge University Press

2. ROBUST FORCE CONTROL OF OPERATOR-MANIPULATOR INTERACTION

As the preliminary study of OMMCS control, a simple man/machine coordinated system shown in Figure 1 has been investigated to obtain useful insights for designing an efficient control system for the OMMCS shown in Figure 2. The preliminary study includes a robust control design and its real time implementation on the man/machine system based on a linear slide that consists of a linear track and a roller carriage. The roller carriage (or slide) is joined to a brushless DC servo motor by a nonslip drive cable system and a force sensor is integrated onto the plate to provide the operator interface.

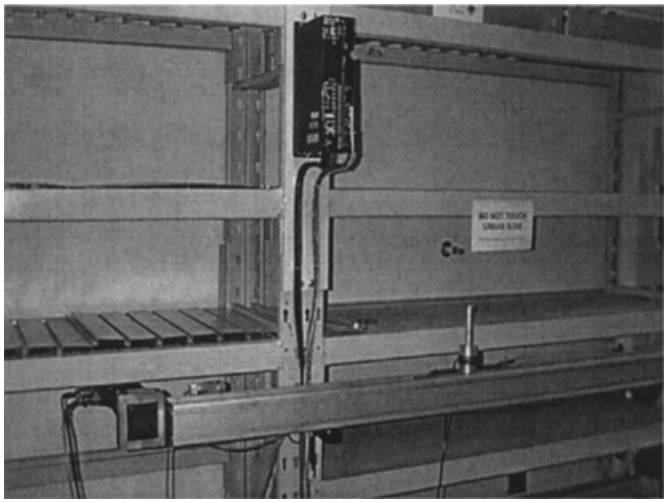


Fig. 1. A simple man-machine coordination system.

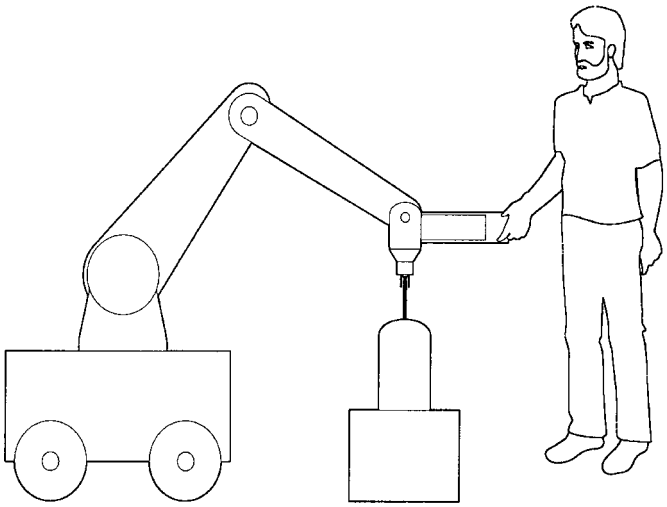


Fig. 2. Operator-mobile manipulator coordination system.

In control design a variation of the hybrid control scheme[7] is adopted. In this approach that utilizes explicit forces, the exact geometry of the surface of the moving object is not required. Therefore, explicit force control is suitable for an OMMCS in which a human operator interacts physically with the robotic system by actually grasping an interface grip (Figure 3).

The nominal explicit force control law is applied as follows:

$$m\ddot{x} = F_d - K_I \int K_e(x - x_d)dt - K_D\dot{x} \tag{1}$$

where m and x are the mass and the displacement of the slide or the roller carriage, respectively, x_d is the motion intention of the operator, F_d is the desired force command, K_e is the resulting environment stiffness of the interactive motion between the operator's arm and the interface handle, K_I and K_D are the integral control gain and the active damping gain, respectively.

The integral control was chosen due to its zero steady state error and low-pass filter characteristics. The active damping term is very effective in maintaining stable contact and avoiding bounces. The desired contact force is set to zero since the ideal system is considered to be a control system designed in such a way that the operator leads a task without feeling any force interaction from the machine.

The force error and the integral-controlled force are weighted by the transfer matrices W_1 and W_2 respectively. Note that the trajectory applied by the human operator is injected to the loop to generate the contact force. The control design is carried out using the Mat-lab Robust Control Toolbox v. 5.1 which solves a weighted mixed sensitivity problem as follows:

$$\max_{\gamma} \left\| \begin{matrix} \gamma W_1 S \\ W_2 T \end{matrix} \right\| < 1 \tag{2}$$

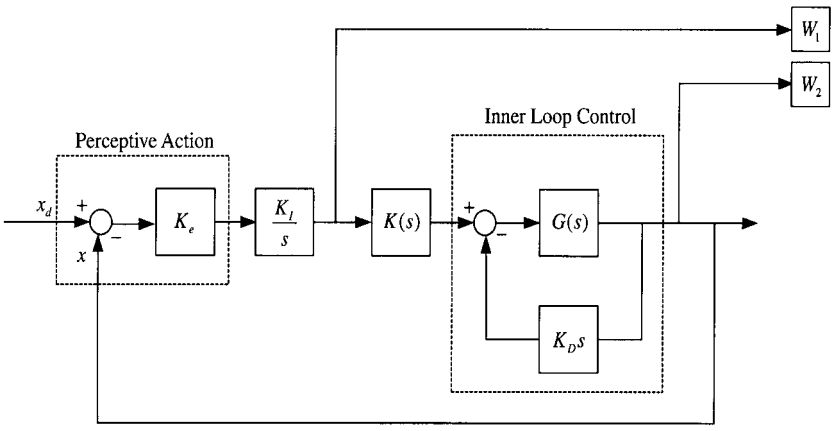


Fig. 3. Robust explicit force control.

https://doi.org/10.1017/S0263574702004113 Published online by Cambridge University Press

where S is the sensitivity function and T is the complementary sensitivity function.

Experimental study was performed to verify the efficacy of the developed robust control law. The operator's motion intention is illustrated in Figures 4a and 5a for the nominal explicit force controller and the robust controller, respectively. The range of each reference motion was marked on the side of the linear slide so that the operator can use his/her visual senses to perform a proper tracking task. The amplitudes of the reference motion are –0.15 m to 0.15 m and –0.175 m to 0.215 m, respectively. It should be noted that the operator is instructed to regulate the interaction force to zero while tracking the reference trajectory. In other words, the human operator plays an important interactive role as a controller utilizing vision and force senses. It is not difficult to see the superior force regulation of the robust controller over the nominal controller by comparing Figures 4b and 5b. It is observed in Figure 5b that the reaction force is bounded to a very small value so that smooth coordination between the human operator and the manipulator is achieved. Note that a faster trajectory with the higher amplitude was applied for the robust controller and Figure 4a represents the force regulation of the nominal (or nonrobust) control with the best tuned feedback gains.

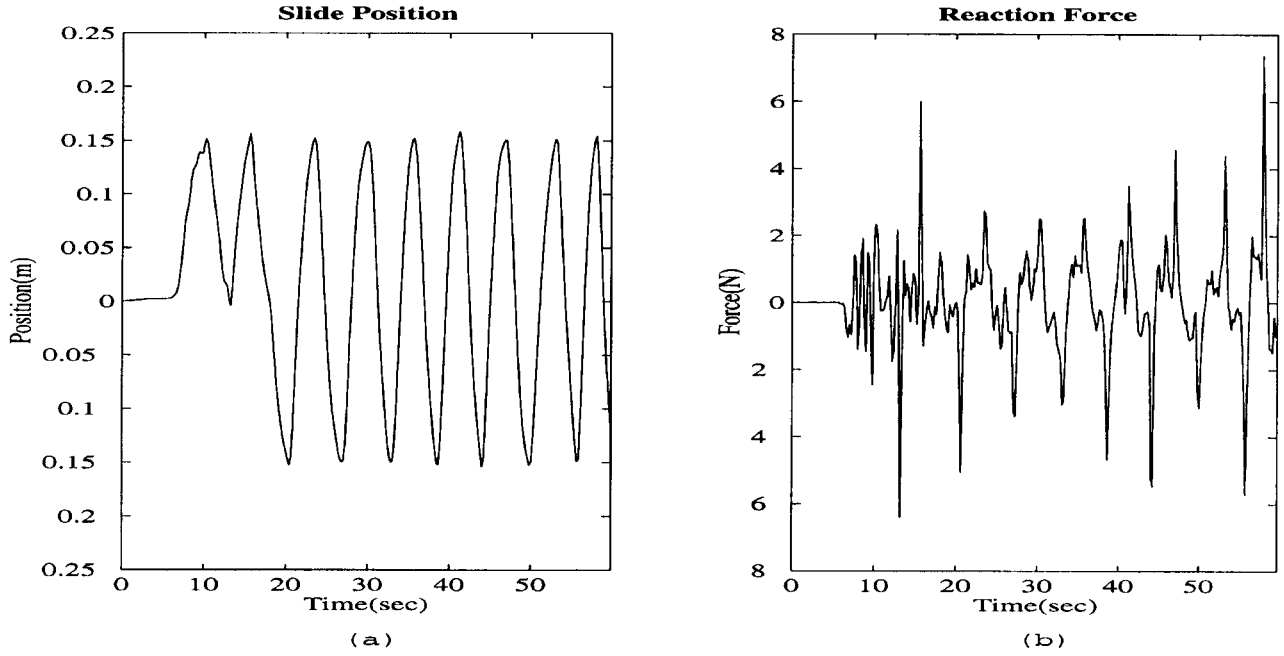


Fig. 4. Tracking and force regulation: nominal control.

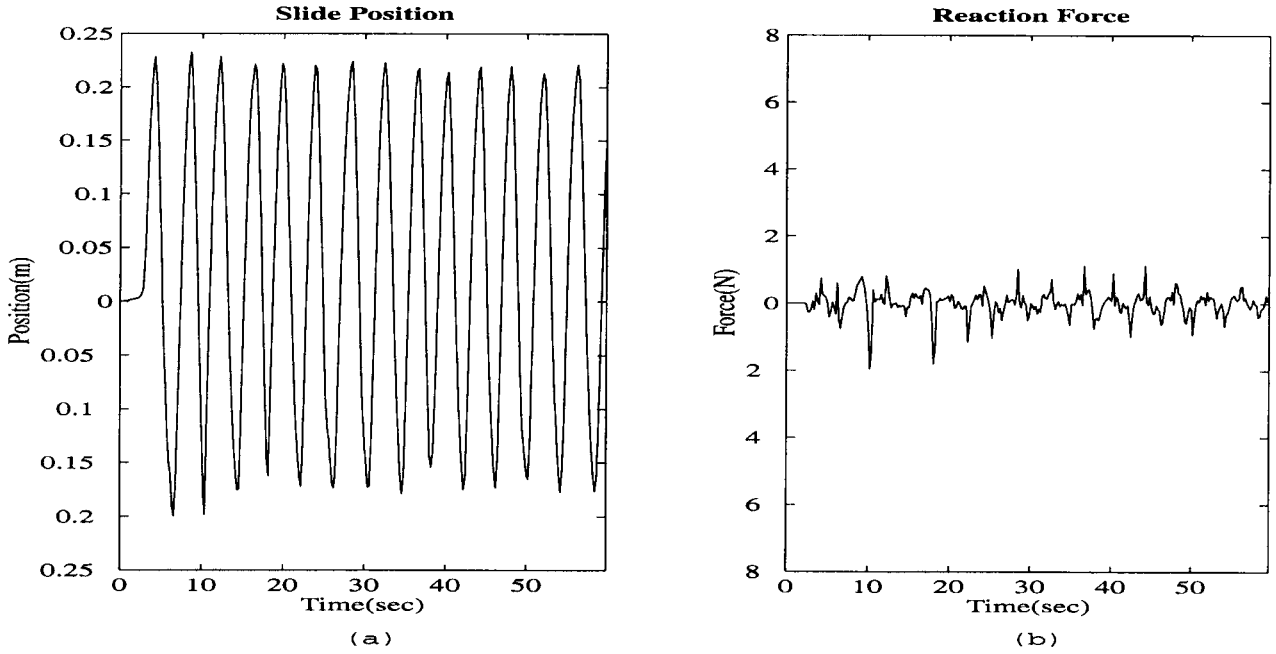


Fig. 5. Tracking and force regulation: robust control.

https://doi.org/10.1017/S0263574702004113 Published online by Cambridge University Press

3. DYNAMIC MODELING OF THE MOBILE PLATFORM

Hong et al.[8] has shown that the nonholonomic (slip free) models are inadequate for differentially driven wheeled mobile robots with any substantial load. By considering slip of the wheeled platform's tires, the assumption of non-holonomic motion is violated. In this section, the dynamic equations of motion are derived using the Newton-Euler method and incorporate Dugoff's empirical based nonlinear tire friction model.[9] The free-body diagram of the mobile platform is shown in Figure 6. For the dynamic equations of motion derived below, the body centered frame for the platform is used as can be seen in the free-body diagram.

The velocity equations of the system are written as

$$u=\frac{1}{2}(u_l+u_r), \tag{3}$$

$$v=\frac{d_2}{d_1}(u_l-u_r)+v^s,\ \omega=\frac{1}{2}(u_l-u_r) \tag{4}$$

$$u_l=r_w\omega_l-u_l^s \text{ and} \tag{5}$$

$$u_r=r_w v_r-u_r^s. \tag{6}$$

where u is the longitudinal velocity, v is the lateral velocity, ω is the yaw rate, v^s is the lateral slip velocity and u_l and u_r are the longitudinal velocities of the wheel centers.

It is not difficult to show that the motion of the reference point X_p to be chosen as the output of the platform controller is described by the following equations:

$$\dot{x}_p=u\cos\theta-d_4\omega\sin\theta-\delta_x, \tag{7}$$

$$\dot{y}_p=u\sin\theta+d_4\omega\cos\theta+\delta_y, \text{ and} \tag{8}$$

$$\dot{\theta}=\omega \tag{9}$$

where $\delta_x=v^s\sin\theta$ and $\delta_y=v^s\cos\theta$.

Then, the equations of motion of the mobile platform can be written as

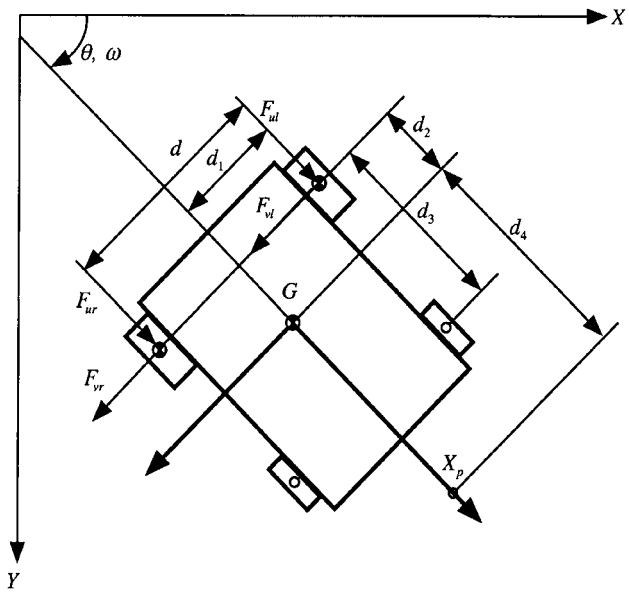


Fig. 6. The mobile platform.

$$\dot{u}=\frac{F_{ul}+F_{ur}}{m_p}+v\omega, \tag{10}$$

$$\dot{v}=\frac{F_{vl}+F_{vr}}{m_p}-u\omega, \tag{11}$$

$$\dot{\omega}=\frac{1}{I_p}[d_1(F_{ul}-F_{ur})-d_2(F_{vl}+F_{vr})], \tag{12}$$

$$\dot{\omega}_l=\frac{1}{I_\omega}(\tau_l-F_{ul}), \text{ and} \tag{13}$$

$$\dot{\omega}_r=\frac{1}{I_\omega}(\tau_r-F_{ur}) \tag{14}$$

where τ_r and τ_l are the control inputs, m_p is the mass of the platform, I_p is the moment of inertia of the platform about z axis, I_ω is the moment of inertia of the combined mass of the wheel and the actuator system about the wheel axis. Note that the equations of motions are not in closed form. F_{ur}, F_{ul}, F_{vr} and F_{vl} are the tire forces acting on the right and left wheels in longitudinal and lateral directions, respectively. similarly, the longitudinal and lateral forces on the wheels are calculated by Dugoff's tire friction model.[9]

Now, the state variables are defined as $\dot{\eta}=[x_p\ y_p\ \theta\ u\ \omega]^T$. Then, the equations of motion can be written in state space form as

$$\dot{\eta}=f(\eta)+g(\eta)\tau+\delta. \tag{15}$$

where δ is the uncertainty vector.

4. MODELING OF THE MANIPULATOR

The model of the manipulator[10] can be described as

$$M(\xi)\ddot{\xi}+C(\xi,\dot{\xi})\dot{\xi}+G(\xi)=\tau_m \tag{16}$$

where ξ is the vector of the joint angles, $M(\xi)$ is the symmetric positive-definite manipulator inertia matrix, $C(\xi,\dot{\xi})\dot{\xi}$ are the Coriolis and centripetal torques and τ_m corresponds to the actuator torques. In this paper, a 3-linked articulate manipulator, as shown in Figure 1, is employed.

5. POSITION-BASED OMMCS CONTROL

The position-based OMMCS control method to be developed implements the coordination scheme utilized in the interaction control scheme[6] and the robust explicit force control developed for the simple operator-manipulator coordination developed in Section 2.

In the interaction control scheme, the manipulator is commanded to follow the desired trajectory in task space and the mobile platform is responsible for positioning the manipulator at a specified point in the workspace to avoid singular configurations of the manipulator. This motivates the application of interaction control to mobile manipulators in which the controllers are independently designed for each subsystem. The desired trajectory of the mobile manipulator is given in the global frame. The manipulator is commanded to move in the local frame fixed on the first joint axis.

https://doi.org/10.1017/S0263574702004113 Published online by Cambridge University Press

Subsequently, the base of the manipulator, which is located on the platform, is followed by the mobile platform in such a manner that it can track the trajectory transformed into the local frame.

In OMMCS control, the motion is initiated by the reference trajectory applied by the operator in the global frame. Then, the manipulator is commanded by the robust force controller developed for the simple coordination system. Subsequently, the base of the manipulator, which is located on the platform, is followed by the mobile platform.

The output X_p associated with Equation (15) is selected as the end point of the mobile manipulator in a nonsingular configuration and defines the new sets of state variables as $x=(x_1\ x_2)^T$, $x_1=(x_e\ y_e)^T$, and $x_2=(\dot{x}_e\ \dot{y}_e)^T$. Then, the transformation of the output equation is performed into the global frame. Differentiating the state vector x, we obtain the dynamic equation in the global frame as follows:

$$\dot{x}=\zeta(\theta, x, \delta)+\Phi(\theta, \delta)\tau+\eta(\theta, x, \delta) \tag{17}$$

When wheel slip is neglected, the equations of motion are obtained as follows:

$$\dot{x}_N=\zeta_N(\theta, x)+\Phi_N(\theta)\tau. \tag{18}$$

Let us denote the following equations:

$$\Phi(\theta, \delta)=\Phi_N(\theta)+\Delta\Phi(\theta, \delta) \text{ and} \tag{19}$$

$$\zeta(\theta, x, \delta)=\zeta_N(\theta, x)+\Delta\zeta(\theta, x, \delta) \tag{20}$$

where $\Delta\zeta$ and $\Delta\Phi$ are the uncertainty terms. Then, $\Delta\Phi$ can be written as

$$\Delta\Phi(\theta, \delta)=\Phi_N(\theta)\tilde{\Phi}(\theta, \delta) \tag{21}$$

$$\Delta\zeta(\theta, x, \delta)=\Phi_N(\theta)\tilde{\zeta}(\theta, x, \delta) \text{ and} \tag{22}$$

$$\Delta\eta(\theta, x, \delta)=\Phi_N(\theta)\tilde{\eta}(\theta, x, \delta). \tag{23}$$

Then Equation (17) is rearranged as

$$\dot{x}=\zeta_N(\theta, x)+\Phi_N(\theta)\tau+\rho(\theta, x, \delta) \tag{24}$$

where $\rho(\theta, x, \delta)=\Phi_N(\tilde{\zeta}(\theta, x, \delta)+\tilde{\Phi}(\theta, \delta)+\tilde{\eta}(\theta, x, \delta))$.

Therefore, the dynamic equations of motion of the mobile manipulator in task space satisfy the matching condition. It is well known that the matching condition is the structural form of a dynamic system to be satisfied for the application of a wide class of robust control algorithms.

Now, the position error and the velocity error are defined as $e_p=x_1-x_1^d$ and $e_d=x_2-x_2^d$. Then, the tracking error dynamics can be described as follows:

$$\dot{e}=Ae+B\{\chi+\eta-\dot{x}_2^d\} \tag{25}$$

where $e=(e_p\ e_d)^T$. The input-output description of Equation (17) is linearized to cancel the nonlinearities using the feedback $\tau=\Phi_N^{-1}(\chi-\zeta)$. Then, the closed loop reduces to $\dot{x}=\chi+\rho$.

The control design to follow is based on the premise that it may be possible to estimate worst case bounds on the effect of wheel slip on the tracking performance of the system. The control law χ is then designed to guarantee stability of Equation (25). The norm bound of the uncertainty term ρ is obtained as

$$\|\rho\|=\|\Phi_N(\tilde{\zeta}+\tilde{\Phi}+\tilde{\eta})\| \le \bar{\rho}. \tag{26}$$

Then, the control system design of the mobile manipulator is equivalent to a design problem of decoupled linear subsystems with the additional feedback as follows:

$$\chi=\dot{x}_2^d-K_d e_d-K_p e_p+\Delta\chi \tag{27}$$

where

$$\Delta\chi=\begin{cases} -\dfrac{\Phi^T P e}{\|\Phi_T P e\|}\bar{\rho}, & \text{for } \|\Phi^T P e\| \ge \epsilon \\ -\dfrac{\Phi^T P e}{\epsilon}\bar{\rho}, & \text{for } \|\phi^T P e\| < \epsilon \end{cases}. \tag{28}$$

The positive definite matrix P is the unique solution to the Lyapunov equation

$$\bar{A}^T P+P\bar{A}+Q=0 \tag{29}$$

where Q is a symmetric positive definite matrix, $\bar{A}=A-BK$, and $K=(K_p\ K_d)$. The control laws (27) and (28) can be easily proven by taking the Lyapunov function $V=e^T P e$.

6. INTERACTIVE FORCE CONTROL OF THE OMMCS

As the first approach to achieve the minimal effect of wheel slip on control performance, a robust position-based controller was designed for the mobile platform. In this section, an alternative control method for the operator-mobile manipulator coordination system (OMMCS) is developed based upon robust impedance control of the platform and robust explicit force control of the operator-manipulator system.

A typical operator-mobile manipulator is comprised of three primary subsystems: a human operator, a mobile platform and a robotic manipulator. The mobile platform is usually designed to have larger mass than the manipulator does due to the consideration of the structural stability of the mobile manipulator. Any nonsmooth motion of the mobile platform can be destructive to the motion of the other subsystems. Therefore, the compliant motion provided by the mobile platform together is expected to reduce the harmful effect of the wheel slip and the dynamic interaction that act as a disturbance to the total system. However, the slip terms that appear in the equations of motion of the platform are not treated explicitly as in the position-based approach. Instead, in this force-based approach, a base force/torque sensor is utilized to implement impedance control so that smooth positioning or nondestructive interaction can be achieved by regulating the dynamic and interactive behavior of the subsystems. The robust force control method developed for the simple coordination system is utilized for controlling the manipulator. Note that the proposed control method is also based on by the interaction control,[6] in which the suitable controllers are independently designed for each subsystem based on a coordination algorithm.

The interactive force control scheme is depicted in Figure 7. The control loop shown in the figure is representative in that it only illustrates the motion of a single axis in task space for simplicity. The position controlled mobile platform is represented by the following equation:

https://doi.org/10.1017/S0263574702004113 Published online by Cambridge University Press

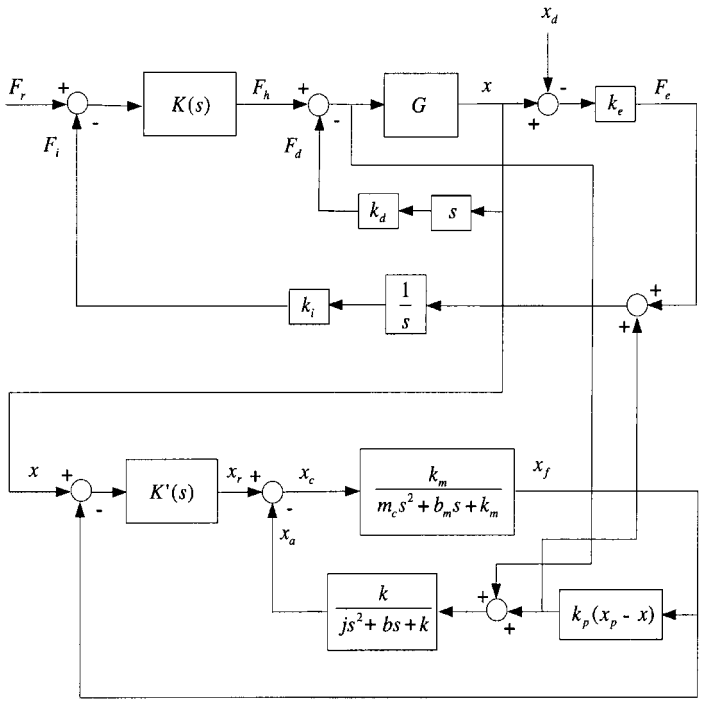


Fig. 7. Interactive force control.

$$\frac{X_f(s)}{X_c(s)} = \frac{k_m}{m_p s^2 + b_m s + k_m} \tag{30}$$

where $K'(s)$ represents a H_∞ controller, b_m and k_m are the feedback gains for the position-controlled platform, m_p is the mass of the mobile platform, X_c is the position command, and X_p is the actual position of the mobile platform. In particular, the position adjustment vector is created by filtering the measured interaction forces and torques to satisfy

$$F = kX_a + b\dot{X}_a + j\ddot{X}_a \text{ via} \tag{31}$$

$$X_a(s) = [k + bs + js^2]^{-1} F(s) \tag{32}$$

where j, b and k represent the design parameters in the impedance controller, F is the measured force, X_a is the position adjustment. With the simplification of diagonal k, b, and j, this reduces to a second order low pass filter for each component of $F(s)$ to generate the respective components of $X_a(s)$ which is added to the nominal trajectory command to produce the overall position command.

The adjustment x_a is added to the nominal trajectory command x without the H_∞ controller to generate the overall position command $x_c = x + x_a$. Note that the reference trajectory of the mobile platform is the actual trajectory of the manipulator x according to the coordination algorithm employed.

7. SIMULATION

The proposed control schemes have been tested by computer simulation. For the dynamic model of the mobile platform (10)–(14), the longitudinal and lateral forces on the wheels are calculated by Dugoff's tire friction model. The longitudinal and lateral tire coefficients, C_x and C_y, are set to 40034 *N/rad* and 40034 *N/rad*, respectively.

The parameters used in this simulation are as follows:

$m_p = 500$ kg, $m_1 = 20$ kg, $m_2 = 20$ kg, $m3 = 20$ kg,
$L_1 = 0.4$ m, $L_2 = 0.4$ m, $L_3 = 0.4$ m

where m_p is the mass of the platform, m_i, I_i and L_i are the mass, the moment of inertia, and the length of the i-th link. The reference trajectories used in the simulation is as follows:

$$x_d(t) = 0.5 + \frac{t}{10} \tag{33}$$

$$y_d(t) = 0.1 \sin \frac{t}{8} \tag{34}$$

$$z_d(t) = 1.0 + 0.1 \sin \frac{t}{6} - 0.1 \sin \frac{t}{3} \tag{35}$$

Figure 8 shows the response of the force/robust position control or the force controller designed for the manipulator and the robust position controller for the mobile platform. The control performance can be further improved by applying H_∞ control to the manipulator and the platform. Figure 9 depicts the control performance of the robust force/robust impedance control system. The position error and the actual output are weighted in designing a robust impedance controller for the mobile platform. The robust controller clearly outperforms the nonrobust controller in tracking as illustrated in Figure 8. It is observed that the tracking error

https://doi.org/10.1017/S0263574702004113 Published online by Cambridge University Press

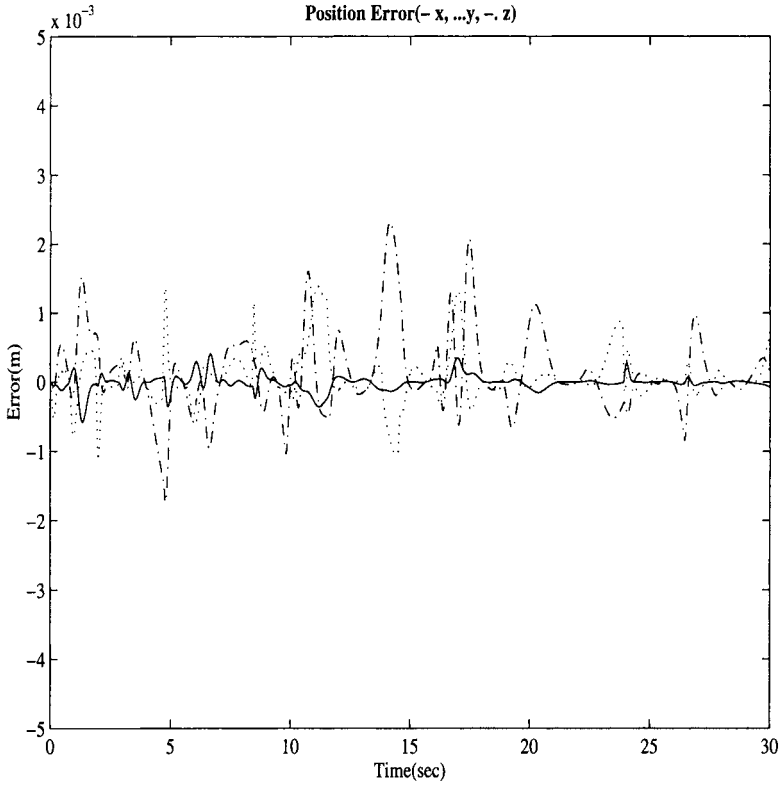


Fig. 8. Tracking: force/robust position control.

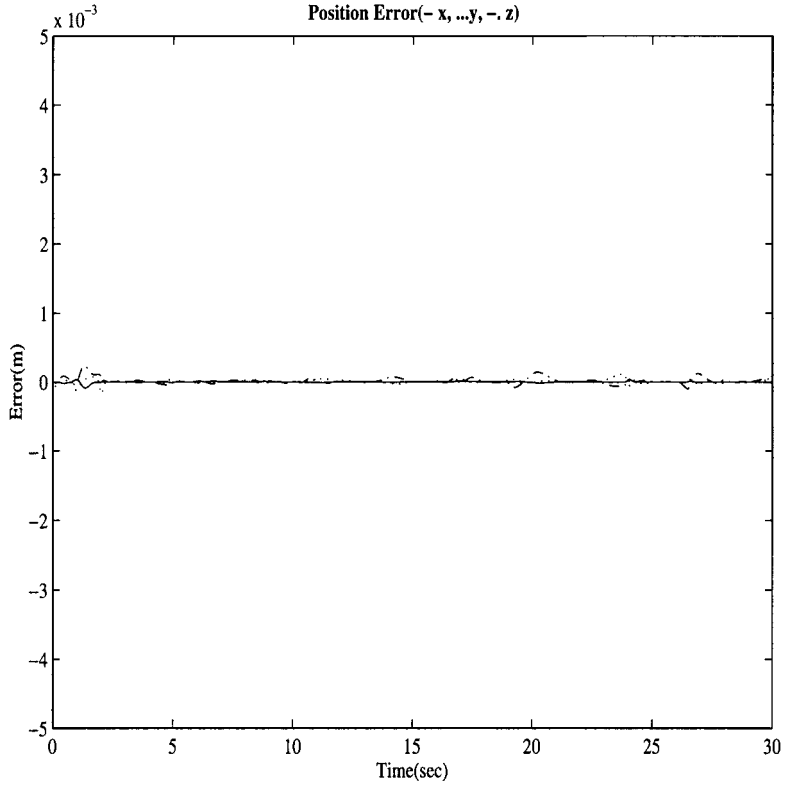


Fig. 9. Tracking: robust force/robust impedance control.

is bounded to a very small value. Note that all the plots illustrated for the control performance shows the best tuned performance of the controller. It is apparent that the tracking performance improved significantly with the impedance control action based on the base force/torque sensor.

8. CONCLUSION

Based on the study for a simple man/machine coordination system, a new coordination control called an interactive force control scheme was developed for an operator-mobile manipulator coordination system (OMMCS) based on a

https://doi.org/10.1017/S0263574702004113 Published online by Cambridge University Press

base force/torque sensor. In the interactive force control scheme, a robust force control of the manipulator and impedance control of the mobile platform are integrated to achieve nondestructive interaction between the operator, the manipulator and the mobile platform. Also, a robust position control was developed to minimize the effect of wheel slip on control performance. In simulation, the developed methods are compared in terms of control performance on following the operator's motion intention. Simulation results show the advantage of the interactive force control that utilizes the impedance control based on a base force/torque sensor.

References

1. T. Fukuda, Y. Fujisawa, and F. Arai, "Man-robot cooperation work type of manipulator", *8th Ann. Conf. of Robotics Society of Japan* (1990), pp. 655–656.
2. H. Kazerooni, "Human-robot interaction via the transfer of power and information signals", *IEEE Transactions on Systems, Man, and Cybernetics* **20**(2), 450–463 (1990).
3. O. M. Al-Jarrah and Y. F. Zheng, "Arm-manipulator coordination for load sharing using compliant control", *Proceedings of IEEE International Symposium on Intelligent Control* (1996), pp. 1000–1005.
4. K. Kosuge, Y. Fujisawa and T. Fukuda, "Control of a man-machine system interacting with the environment", *Advanced Robotics* **8**(4), 427–440 (1994).
5. Y. Yamamoto, H. Eda and X. Yun, "Coordinated task execution of a human and a mobile manipulator", *Proceedings of IEEE International Conference on Robotics and Automation* (1996), pp. 2184–2192.
6. J. H. Chung, S. A. Velinsky and R. A. Hess, "Interaction control of a redundant mobile manipulator", *Int. J. Robotics Research* **17**(12), 1302–1309 (1998).
7. M. H. Raibert and J. J. Craig, "Hybrid position/force control of manipulators", *Transactions of the ASME Journal of Dynamic Systems, Measurement, and Control* **103**(2), 126–133 (1981).
8. D. Hong, S. A. Velinsky and X. Feng, "Verification of a wheeled mobile robot dynamic model and control ramifications", *Transactions of the ASME Journal of Dynamic Systems, Measurement, and Control,* **121**(1), 58–63 (1998).
9. H. Dugoff, P. Fancher and L. Segal, "An analysis of tire traction properties and their influence on vehicle dynamic performance", *SAE Transaction* 1219–1243 (1970).
10. M. W. Spong and M. Vidyasagar, *Robot Dynamics and Control* (Wiley, 1989).

https://doi.org/10.1017/S0263574702004113 Published online by Cambridge University Press